ELSEVIER

Biophysical Chemistry 86 (2000) 119–129

Biophysical Chemistry

www.elsevier.nl/locate/bpc

A universal thermodynamic approach to analyze biomolecular binding experiments ☆

Gerhard Schwarz*

Department of Biophysical Chemistry, Biocenter of the University of Basel, Klingelbergstr. 70, CH-4056 Basel, Switzerland

Received 17 December 1999; accepted 3 February 2000

Abstract

Binding processes of any kind can be characterized as an association of a given ligand with some binding factor. This includes macromolecules as well as supramolecular aggregates such as micelles or membranes. The underlying molecular binding mechanism may be more or less complicated due to various intermediate steps (involving for instance conformational changes, aggregation, cooperativity, etc.). A sensible discussion of possible binding models naturally calls for a model-independent access to basic thermodynamic properties. The present contribution will demonstrate how this can quite generally be accomplished by a pertinent processing of properly selected experimental data. The method requires a series of titration measurements comprising the use of variable amounts of both the ligand and the binding factor. It leads to a linear mass conservation plot (i.e. amount of the ligand vs. a matching amount of the binding factor) whose slope and ordinate intercept are equal to the binding ratio (i.e. bound ligand per binding factor) and the free ligand concentration, respectively. This establishes the specific binding isotherm. The approach also reveals latent structurally determined features of the applied physical measuring signal. A number of examples including specific binding, unspecific adsorption and insertion in two-dimensional molecular films will illustrate the methodology.

Keywords: Binding isotherms; Macromolecules; Liposomes; Monolayer insertion; Ligand partitioning; Signal intensities

1. Introduction

Binding in a most general sense does actually comprise a wide range of somewhat diverse phenomena. In any case, however, there is a certain agent, A, being a potential ligand that will associate with a material binding factor, B. Prominent exponents of the latter moiety are biological macromolecules such as proteins or nucleic acids. They may feature structurally defined specific binding sites. Each of them can either be occupied by the ligand or be vacant. If

☆ Dedicated to Heini Eisenberg.

* Tel.: +41-61-267-2200; fax: +41-61-267-2189.
E-mail address: gerhard.schwarz@unibas.ch (G. Schwarz).

0301-4622/00/$ - see front matter
PII: S0301-4622(00)00128-9

all these sites are equivalent and independent, relevant experimental data may be analyzed toward the thermodynamic binding constant and the number of binding sites in terms of a linear Scatchard plot [1]. Since this presumes a most simple binding model, such an approach is susceptible to substantial misinterpretations in practice [2]. In addition to the lack of sufficient measuring data at high and low saturation, different classes of binding sites as well as cooperative interactions have to be taken into account. This has serious implications regarding the shape of a Scatchard plot [3].

Furthermore, one has to bear in mind that very frequently the ligand A does not really occupy a defined binding site but simply adheres to B owing to rather unspecific forces, particularly caused by electrostatic and/or hydrophobic interactions. Naturally no definite number of binding sites can then be specified. A classical example is the unspecific binding of proteins to nucleic acids where one bound ligand molecule covers a number of binding contacts presented by the nucleotide subunits (of any kind). This implies the possible occurrence of vacant gaps between bound ligand that are too narrow to accommodate one whole ligand molecule. The so induced apparent negative cooperativity may be counteracted by sufficient positive cooperativity exerted between bound ligand as quantitatively described by the basic model of McGhee and von Hippel [4]. Such an analysis of multiple contact binding can be extended to cases involving mutually excluding two or more different binding modes [5,6]. In unspecific binding like that one should rather consider the association of A with B as a partitioning process where the binding factor functions as another solvent (in addition to the basic solvent, usually an aqueous buffer). This binding actually results from solvation effects exerted by B on A. Mutual interactions (being attractive or repulsive) between bound solute A are to be described in terms of thermodynamic activity coefficients.

The present view of binding must be especially adopted when the binding factor is not provided by macromolecules but by large supramolecular aggregates, e.g. micelles, lipid mono- or bilayers, respectively. Even biomembranes can be discussed along these lines according to the 'fluid mosaic model' [7]. In these cases a ligand may not only adhere to the mere outside of such an aggregate but could possibly be incorporated into its interior. Nevertheless all of the present phenomena are to be subsumed in a most general concept of biomolecular binding. Fundamental theoretical and experimental approaches can be carried out in essentially the same way no matter which kind of binding mechanism is involved.

At equilibrium any given binding system can be quantitatively characterized by a pertinent thermodynamic association isotherm (i.e. the 'binding curve'). This implies an unambiguous functional relationship between bound ligand per amount of binding material and the concentration of free ligand. It is determined by the underlying molecular binding mechanism. In order to elucidate that mechanism the binding curve should naturally be evaluated from relevant experimental data in a model-free way. The present contribution will show how this can be accomplished under most general circumstances. The approach takes advantage of a selective series of measured physical binding signals at sufficiently different total concentrations of the ligand and the binding factor. From these data linear mass conservation plots may be constructed whose slope and intercept provide the binding curve variables. Also other useful information regarding individual signal intensities would possibly be available to assess structural conversions. Those results lay a foundation for a subsequent unbiased attempt to analyze the actual binding mechanism.

2. Theoretical

We consider a general binding system comprising a ligand A and the binding factor B which are immersed in a basic solvent at total concentrations c_A and c_B, respectively. Temperature and external pressure are kept constant (isothermic conditions). In the absence of further external variables of state it follows from thermodynamic principles that under equilibrium conditions any of the intensive variables of state in the system is

functionally related to just one independent variable being arbitrarily chosen among the total of such intensive variables. This includes for instance the overall binding ratio, $r = c_{Ab}/c_B$ (c_{Ab}: concentration of bound A) and the free ligand concentration, c_{Af}. Accordingly we have at any rate a definite functional relationship, the binding isotherm

$$r = f(c_{Af}) \tag{1}$$

This applies irrespective of the possibility that bound and/or free ligand molecules assume any number of different structural states. Their individual binding ratios or concentrations, respectively, being also intensive variables of state, will naturally depend on only one independent variable being selected at discretion, e.g. r or c_{Af}. A more detailed thermodynamic argumentation can be found in Appendix A.

Mass conservation always implies the trivial condition

$$c_A = r \cdot c_B + c_{Af} \tag{2}$$

regarding the partitioning of A between bound and free states. This suggests that experiments with a variety of different c_A, c_B pairs are to be conducted in such a way that they provide data at the same level of r and c_{Af}. Then a plot of c_A vs. c_B must result in a straight line whose slope and ordinate intercept would be equal to r and c_{Af}, respectively. How this unbiased approach to the relevant binding curve can be implemented practically will be demonstrated in the following with several experimental systems and measuring techniques. In any case it needs a physical measuring signal that changes upon binding and can be converted to a quantity functionally related to r.

3. Linear binding signals

3.1. Fundamental relations

A commonly adopted experimental routine to monitor binding takes advantage of some property Φ (e.g. fluorescence intensity, circular dichroism) that changes upon a conversion from a free to a bound state. Ordinarily this signal is linearly related to the individual concentrations as expressed by

$$\Phi = \varphi_o \cdot c_{Af} + \sum_i \varphi_i \cdot c_{Ai} \tag{3a}$$

The coefficient φ_o is assumed to be the same for any possible free substrate state (as to be tested without added B). Different states of bound ligand at concentration c_{Ai} ($i = 1, 2, \ldots$) may give rise to different signal intensities φ_i. By applying mass conservation, Eq. (3a) can be converted to

$$\Delta\Phi/c_B = \sum_i \Delta\varphi_i \cdot r_i \quad (\Delta\Phi = \Phi - \Phi_o;\ \Phi_o = \varphi_o \cdot c_A;\ \Delta\varphi_i = \varphi_i - \varphi_o;\ r_i = c_{Ai}/c_B) \tag{3b}$$

which must be a function of the single variable r (since each r_i is an intensive variable of state by itself that depends on r as pointed out above). Accordingly one may measure the present quantity $\Delta\Phi/c_B$ as it changes with c_B for a number of different c_A and collect pairs of c_A, c_B where that quantity is on the same level. These data can then be used for a mass conservation plot to determine the respective r and c_{Af}. This basic idea was independently proposed in 1987 by two groups who applied it to protein–nucleic acid binding [8] and peptide–liposome interaction [9], respectively. It was, however, widely disregarded so far.

In the present article it is to be shown that the underlying concept can be universally extended to all kinds of macro- and supramolecular binding systems. The results will provide latent quantitative features toward a pertinent analysis of the relevant reaction mechanism.

Starting with a given solution of pure A (signal Φ_o) the following titration procedure is proposed where one records the change of Φ upon added B. The normalized signal

$$F = \Delta\Phi/c_A \tag{4a}$$

is then plotted vs. the ratio of total concentrations, c_B/c_A. This is to be repeated with several sufficiently different c_A-values resulting in a

bunch of curves for

$$F = F_\infty \cdot r \cdot (c_B/c_A) \tag{4b}$$

[as derived from Eq. (3b)] where

$$F_\infty = \Sigma_i \Delta\varphi_i \cdot x_i \tag{4c}$$

involving x_i $(= r_i/r)$, the molar fraction of bound A in state i. In simple cases, with only one bound state or if φ_i is always the same, F_∞ would be constant and equal to the signal that is asymptotically approached in the limit of $(c_B/c_A) \to \infty$. Then F/F_∞ will be equal to the molar fraction of bound A, i.e. c_{Ab}/c_A. Generally, however, F_∞ may change as a function of r due to induced transitions between bound states with different signal intensities φ_i. It would thus reveal useful information about the underlying molecular binding mechanism.

In order to exploit the bunch of F vs. c_B/c_A curves we introduce a quantity $Q = F/(c_B/c_A)$ which can be readily extracted from the plotted data. On the other hand, Eq. (4b) implies

$$Q = F_\infty(r) \cdot r \tag{5}$$

so that all points coming under the same value of Q necessarily contribute a c_A, c_B pair for a mass conservation plot according to Eq. (2).

3.2. A model demonstration

The suggested procedure is to be illustrated in Fig. 1 by a practical example involving a simulation of F vs. c_B/c_A data. It is based on an artificial binding model where a linear signal (say fluorescence emission for instance) had been measured in a titration of ligand A solutions with the binding factor B. First of all a series of four

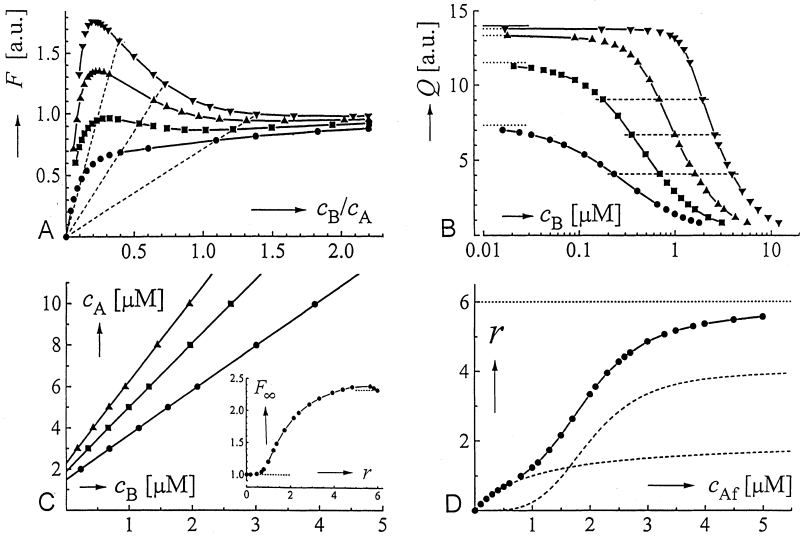

Fig. 1. Processing of simulated measuring data for a binding system comprising a ligand A and a macromolecular binding factor B. (a) The measurements refer to a titration of various different ligand concentrations with component B where $c_A/\mu M = 2$ (●), 3 (■), 5 (▲), 10 (▼). The reduced signal F [see Eq. (4a)] is plotted vs. the total B/A ratio. Dashed lines exemplify a constant value of Q (see text) where the binding curve variables are invariant ($Q = 0.71$, 1.71, 4.08, respectively). (b) Data of panel (a) after their conversion into the more practical direct plot of Q vs. the total concentration of B ($Q = 4.08$, 6.70, 9.03, respectively, at the dashed lines). Limits at low c_B are marked by dotted lines. There is an absolute upper bound of $Q \to 14.0$ for $c_A \to \infty$. (c) Mass conservation plots for the specified Q-levels of panel (b). The inset shows the change of F_∞ upon an increasing extent of binding (lower and upper dotted lines at 1.0 and 2.33, respectively). (d) Binding curve resulting from a sufficient multitude of mass conservation plots. The dashed curves reflect a deconvolution into two separate binding modes that make up the underlying overall binding mechanism (see text).

curves for sufficiently different c_A is presented. Dashed lines through the origin indicate the data where selected values of Q remain constant. Measured points on such a line have equal r and c_{Af} values. They can then be used for a mass conservation plot. It is, however, recommended to plot Q directly from the original data as a function of c_B. Here one obtains horizontal dashed lines that reflect a level of constant Q, r and c_{Af}. Apparently there exist limiting values of Q at low c_B. They decrease for smaller c_B implying that sufficiently large c_A are needed for a mass conservation plot at higher binding ratios. Also one should note a potentially increasing experimental uncertainty in the lower and higher c_B-ranges where the curves tend to level off. Accordingly their intermediate steeper parts would in practice be most suitable to reduce error margins.

Mass conservation plots derived for selected Q-levels are shown together with a plot of F_∞ vs. r [calculated by means of Eq. (5)]. That latter curve clearly indicates a change of the signal intensity upon increasing binding ratios, which is apparently caused by a transition in the binding mode. The resulting overall binding isotherm exhibits an initial part up to approximately $r = 0.75$ that has a hyperbolic shape and complies with a linear Scatchard plot reflecting two binding sites whose binding constant is 10^6 M^{-1}. This part of the total binding isotherm has been continued by the given dashed curve. The other dashed curve represents the remaining difference with the total binding curve. Its sigmoidal course suggests positive binding cooperativity. With an apparent number of four binding sites one obtains a Hill coefficient of 4 and a cooperative binding constant per site of $5 \cdot 10^5$ M^{-1}. Thus one can quantitatively deconvolute the given titration data in terms of the present two binding modes $i = 1$ (non-cooperative) and $i = 2$ (cooperative). Then one has according to Eq. (4c)

$$F_\infty = \Delta\varphi_1 \cdot (r_1/r) + \Delta\varphi_2 \cdot (r_2/r) \qquad (6)$$

From the given data it follows in the limit of $r \to 0$ ($r_1 \to r$, $r_2 \to 0$) $F_\infty \to \Delta\varphi_1 = 1.0$ while in the other extreme $r \to 6 \cdot 10^{-2}$ (i.e. $r_1 \to 2 \cdot 10^{-2}$, $r_2 \to 4 \cdot 10^{-2}$) and $F_\infty \to 2.33$ so that a value of $\Delta\varphi_2 = 3.0$ can be evaluated. Thus the cooperative binding mode is associated with a threefold increase of its individual signal intensity. This may be interpreted in structural terms depending on the physical nature of the signal. Subsequent to this general demonstration of the present approach its practical use is to be discussed with some applications to actual experimental systems.

3.3. Protein–nucleic acid interaction

This considers previous data with protamine peptides binding to DNA [10]. They had been analyzed quite satisfactorily using a theoretical treatment [11] based on the McGhee–von Hippel model [4]. It was done in view of a presumed large binding site of the peptide molecule (20 amino acid residues, most of them being positively charged arginines). Now a model-free data processing routine is to be performed leading to the relevant thermodynamic binding isotherm as depicted in Fig. 2. The protamine carried a fluorescein label that was quenched upon binding. Accordingly the fluorescence decrease per peptide concentration can be taken as a suitable linear signal. There is an apparent maximum $Q_{max} = 0.76$ (limiting slope of the data) that indicates full saturation of binding. An upper bound of F resulting from a constant level of F_∞ is not directly accessible from these measurements but has been evaluated in the course of the present evaluation procedure. A conversion of the available data into a number of Q vs. c_{DNA} plots provides c_{PA} (total protamine concentration) vs. c_{DNA} for mass conservation analysis. Applying Eq. (5) it turns out that $F_\infty = 14.1$ ($\pm 1\%$) remains actually constant. In other words, there is no structurally mediated change of fluorescence quenching upon a variation of the binding ratio. The resulting binding curve reflects a highly cooperative nature with a Hill coefficient of approximately 20. The apparent limit of $r = 5.7 \cdot 10^{-2}$ as well as Q_{max}/F_∞ can be utilized to calculate the size of a protamine binding site. This results in a value of 18 (± 0.5) nucleotide units.

3.4. Membrane active peptides

The method under consideration can also be usefully employed in cases where the binding

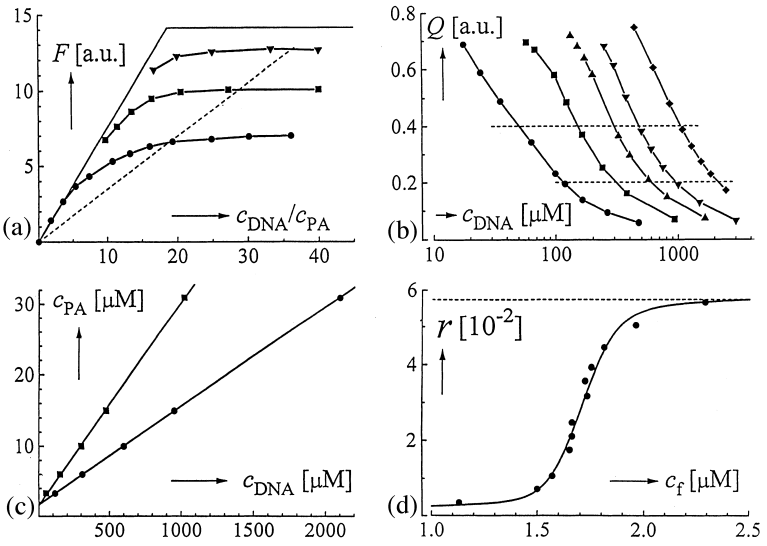

Fig. 2. Protamine peptide (PA) binding to DNA. (a) Original data (fluorescence decrease per peptide) based on the quenching of a fluorescent label [10]. The peptide concentrations (in μM) are 3.3 (●), 6.0 (■) and 15.0 (▼), respectively. Intersection points with the dashed line have the same Q-value. The obtuse-angled solid line (limited by Q_{max} and F_∞) reflects the asymptotic course of the data at $c_{PA} \to \infty$. (b) The more appropriate plots of Q vs. c_{DNA} (in terms of nucleotide residues) are shown together with two additional ones, $c_{PA}/\mu M = 10$ (▲), 31 (◆). (c) Mass conservation plots for $Q = 0.2$ (●), and 0.4 (■) as marked by the dashed lines in panel (b). (d) Resulting binding curve (see text).

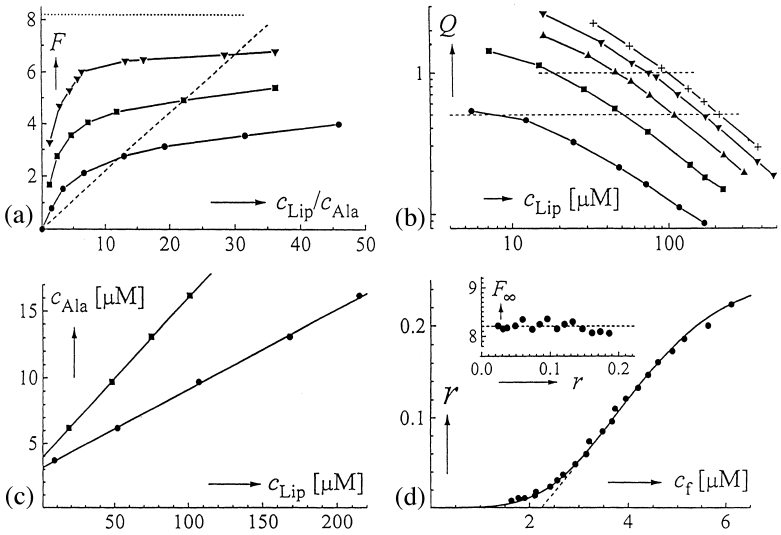

Fig. 3. The case of alamethicin binding to DOPC small unilamellar vesicles (SUV). (a) The signal is the peptide's negative molar ellipticity at 224 nm (10^3 deg cm^2/dmol) recorded for $c_{Ala}/\mu M = 3.7$ (●), 6.2 (■), 13.1 (▼). (b) The Q vs. c_{Lip} plots with additional two $c_{Ala}/\mu M = 9.7$ (▲), 16.2 (+). Dashed lines at $Q = 0.5$ and 1.0. (c) Mass conservation plots for those specified Q. (d) Binding curve with a critical concentration of $c_f = 2.25$ μM (extrapolated by the dashed line). The inset reveals an invariant F_∞ above the critical concentration.

factor is a supramolecular entity such as a lipid membrane. As an example the partitioning of the channel forming peptide alamethicin between lipid vesicles and their aqueous surroundings may be considered [12,13]. This case is illustrated in Fig. 3. The linear binding signal is a drastic change in the circular dichroism spectrum resulting from an increase in helicity upon association with the lipid bilayer. Appropriate Q vs. lipid concentration plots for given peptide concentrations lead to mass conservation plots for fixed Q resulting in the relevant association isotherm. This could quantitatively be very well interpreted by a model implying a weak incorporation of monomeric peptide that above a certain critical concentration undergoes a strong aggregation. A practically constant value of $F_\infty = 8.25 \cdot 10^3$ deg cm^2/dmol ($\pm 1.5\%$) is apparently only reflecting the peptide aggregates whose secondary structure remains unaltered at increasing degrees of association.

The same peptide had also been studied with a fluorescent label whose emission increases upon its binding to the lipid moiety [9]. This signal may be used in the present approach toward the r vs. c_f curve as shown in Fig. 4a. Apparently the implanted label leads to a substantial increase of the binding affinity reflected by an approximate tenfold decrease of the critical concentration and an initial monomeric partition coefficient of some $7 \cdot 10^4$ M^{-1} (in contrast to approximately 10^3 M^{-1} for the unlabeled peptide). The signal intensity F_∞ drops significantly from approximately 2.0 (presumably due to bound monomers) to values less than 1.5 (indicating an intense quenching in the aggregates).

Positively charged membrane-active peptides do generally not show indications of aggregation as was for instance established for the bee venom factor melitin [14,15] and the mastoparans from various wasp species [16–18]. Some relevant data for mastoparan X [19] are shown in Fig. 4b. In this case molar ellipticities and fluorescence of a Trp residue, respectively, had been utilized as a linear signal. The mass conservation plots for Q (in deg cm^2/dmol) = 400–800 resulted in a practically constant $F_\infty = 14\,900$ deg cm^2/dmol ($\pm 2\%$). This could be utilized to calculate binding curve points [using Eq. (5)] with a number of available isolated Q-values.

4. Surface area signals

4.1. Monolayer thermodynamics

A monomolecular film at some interface may act as a binding factor for certain other molecules which can be integrated in it. This is especially

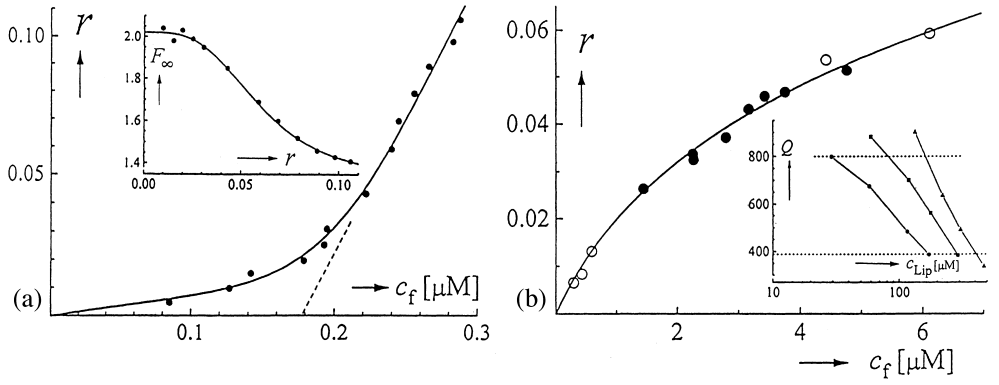

Fig. 4. (a) Binding curve for a fluorescence labeled alamethicin with DOPC-SUV. Initial course of apparently monomer partitioning (linear increase of r) is followed by a steep increase presumably caused by aggregation beyond a critical concentration of $c_f = 0.18$ μM. The inset reflects a drop of fluorescence intensity upon aggregation. (b) Association isotherm of mastoparan X with DOPC-SUV derived from mass conservation plots (negative molar ellipticity in deg cm^2/dmol) for Q between the dashed levels in the inset (full circles). The open circle points have been calculated with the observed constant F_∞ (see text).

interesting for studies on the incorporation of bioactive substances in a lipid monolayer that serves as a basic model of a membrane. Experimentally such binding may be investigated on an air/water interface in a conventional Langmuir trough. From a thermodynamic point of view the surface pressure π (i.e. the induced decrease of the aqueous surface tension) must be introduced as another independent variable of state (in addition to temperature T and external pressure p). Accordingly all intensive equilibrium properties of the system are functionally controlled by the binding ratio (or interfacial mixing ratio, respectively) $r = n_{Am}/n_L$ (i.e. amount of monolayer inserted agent per amount of lipid) and π (when T and p are kept constant). In other words, these two quantities are the only independent variables of state of the whole monolayer/subphase system (see Appendix A for a more detailed argumentation). This may be taken advantage of to determine the partitioning of total component A between the lipid monolayer (n_{Am}) and the aqueous subphase (n_{As}) by means of the mass conservation law:

$$n_A = r \cdot n_L + n_{As} \tag{7}$$

Any intensive variable other than r and π are functionally determined by these two variables. This applies for instance to the monolayer area, A, per amount of lipid

$$A^* = A/n_L = f(r,\pi) \tag{8}$$

Thus measurements under conditions of the same values of A^* and π refer to invariant values of r which naturally also keeps the subphase concentration, $c_{As} = n_{As}/V$, on a constant level. If the subphase volume V is not changed in the experiments, r and n_{As} in Eq. (7) would thus be invariant in case we collect data for n_A and n_L where π and A^* are fixed. Then a mass conservation plot of n_A vs. n_L must be a straight line whose slope and ordinate intercept directly result in r and n_{As}. This is to be repeated for a sufficient number of A^*-values. Then the partitioning (or 'binding') isotherm can be constructed for a given lateral pressure π. Also the molecular area requirement of inserted A can so be evaluated as a function of π and r [20].

4.2. Insertion in lipid films

The underlying practical procedure with A^* being the pertinent measuring signal will be illustrated in Fig. 5. Some relevant results are presented for a monolayer of POPC (palmitoyloleoylphosphatidylcholine) to which another lipid, namely DCPC (dicaproylphosphatidylcholine), is added [Dumas and Schwarz, unpublished data]. Pure POPC forms an insoluble monolayer at the air/water interface [21]. The DCPC is less hydrophobic (due to its much shorter C_{10}-hydrocarbon chains) so that the question arises whether it may to some degree desorb into the subphase, particularly if the monolayer has been subjected to higher surface pressures. To this end a series of classical pressure–area isotherms are recorded (π vs. A^*) where n_{POPC} is the same and n_{DCPC} is successively increased (isothermic titration). For a given π the increase of A^* can be determined as a function of the added n_{DCPC}. Since A^* is always the same for a pure lipid monolayer one may simply plot ΔA^* vs. n_{DCPC} according to the example being presented. Points at the same level of ΔA^* correspond to equal values of r and n_{DCPCs}. The respective total amounts n_{POPC} and n_{DCPC} can thus be used for mass conservation plots such as those being displayed. In that case finite intercepts on the ordinate are obtained implying a non-negligible desorption of the colipid in the subphase. The resulting binding/insertion isotherm exhibits an apparently linear course. This implies a constant partition coefficient $K_p = r/c_{DCPCs}$. It is found to increase at decreasing surface pressure so that below approximately 20 mN/m practically no more desorption occurs.

The insertion of less chemically related agents into a lipid monolayer may be subject to more complex features. This turned out to be the case for the HIV-1 fusion peptide when interacting with a POPC monolayer [20]. The results of an isothermic titration are displayed in Fig. 6. Of special interest would be the insertion in a reasonably compressed monolayer at lateral pres-

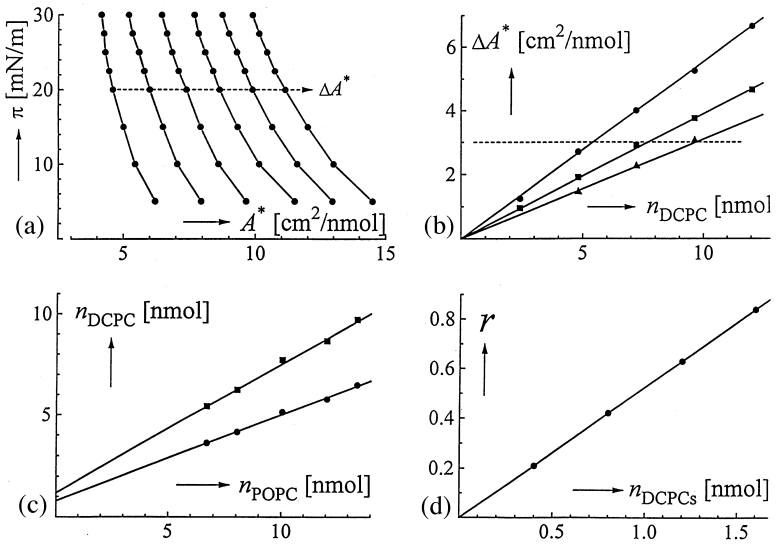

Fig. 5. Insertion of DCPC in a POPC film. (a) Surface pressure–area isotherms for 8.05 nmol of pure POPC (extreme left curve) to which successively DCPC is added in steps of 2.4 nmol (from left to right). At a given pressure (dashed line) the induced increase of A^* can be obtained. (b) Increase of area per lipid at 30 mN/m for n_L/nmol = 8.05 (●), 10.05 (■), 13.4 (▲), respectively. The dashed line indicates a level of constant r and n_{DCPCs} (subphase desorbed DCPC). (c) Mass conservation plots for 30 mN/m and ΔA^* (in cm^2/nmol) = 2 (●), 3 (■). (d) Resulting insertion isotherm for 30 mN/m.

sures that mimic the physical properties of a biological cell membrane. Under these circumstances measurable amounts of the peptide are driven into the subphase as reflected by the mass conservation plots at 25 mN/m. The resulting binding curves reveal a peculiar shape that indicates substantial structural transitions of the peptide–lipid arrangements in the monolayer. There is especially a sharp bend at a critical value of the binding ratio, r_{crit}, that can also be seen in the course of A^* vs. r. This suddenly appearing dramatic increase of the peptide's molecular area requirement may possibly be caused by the formation of water-filled pores.

5. Conclusions

The partitioning of a ligand between its free and bound states can be generally determined in the proposed model-free way. It involves a linear mass conservation plot whose slope and ordinate intercept are equal to the binding ratio r and the free ligand concentration, c_f, respectively. The required c_A, c_B-data (of matching total ligand and binding factor concentrations) are available from a series of titrations where an appropriate measuring signal determines a level of constant r and c_f. In addition to the binding curve (r vs. c_f) further structural information may be obtained from the observed change of the measuring signal with r. The so obtained results are then to be discussed with respect to the underlying molecular binding mechanism.

Acknowledgements

Our experimental work was always supported by the Swiss National Science Foundation, most lately by Grants No. 21-52127.97 and No. 31-042045.94.

Appendix A: Thermodynamic principles

A given material system that is possibly be subject to surface activity may be considered at constant temperature and external pressure. Under equilibrium conditions its Gibbs free energy

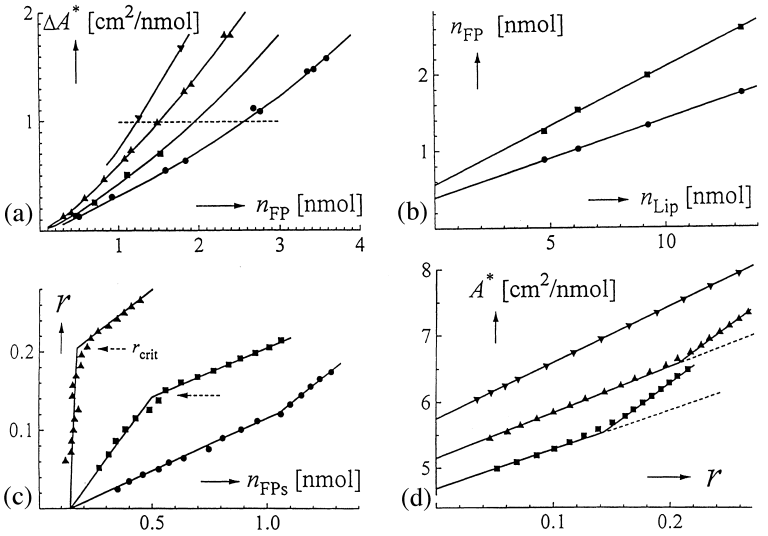

Fig. 6. A viral fusion peptide in a compressed lipid monolayer. (a) Increase of film area per lipid at 25 mN/m upon added peptide for various lipid amounts: n_{Lip}/nmol = 4.75 (▼), 6.2 (▲), 9.25 (■), and 13.35 (●). (b) Mass conservation plots for ΔA^* (in cm^2/nmol) = 0.6 (●), 1.0 (■). (c) Insertion isotherms for π (in mN/m) = 18 (▲), 25 (■), 32 (●). Dashed arrows indicate an apparent critical mixing ratio. (d) Change of the measuring signal A^* with the insertion ratio for given pressures (in mN/m) = 10 (▼), 18 (▲), 25 (■). The sharp bends occur at the r_{crit} of the insertion isotherms shown in panel (c).

G will then change according to the total differential

$$dG = \Sigma_i \mu_i dn_i + \gamma dA \quad \text{(A1)}$$

assuming a number of material components with amounts (i.e. mol numbers) n_i ($i = 0, 1, 2, \ldots$) and a possible surface activity resulting from a surface tension, γ, at an interfacial area A; μ_i stands for the relevant chemical potentials. This implies that G as well as any of its partial derivatives is a function of the individual n_i and A. These quantities are extensive variables of state which are proportional to the extent of the system (in terms of volume, material amount, etc.). Intensive variables such as μ_i and γ or π, respectively (being independent of the system's extent) will only depend on the ratios of n_i, A with regard to some other suitably chosen extensive variable.

In case of the binding factor B and all bound ligand states A_i the relevant ratios may be taken as $r_i = n_i/n_B$, and $A^* = A/n_B$. Actually there may be only one ligand which merely exists in different structural manifestations A_i (conformations, aggregated monomers, etc.) which can convert into each other. Then the equilibrium condition ($dG = 0$) implies that all the individual μ_i must be equal. This results in equations between the r_i which (in addition to mass conservation) establishes a relationship to express r_i as a function of r ($= \Sigma_i r_i$) according to a general mass action law. In other words, the thermodynamic properties of the binding factor phase (with its bound ligand) are solely controlled by r and (if applicable) A^*.

An analogous argumentation goes for the free solution phase where a surface term is not needed. The relevant intensive variables are defined with respect to the volume V. Thus molar concentrations $c_i = n_i/V$ will determine the individual chemical potentials. These must be equal for one ligand in different possible states. Then $c_f = \Sigma_i c_i$ becomes a single independent variable of the free solution system.

Now a possible partitioning equilibrium between the binding factor and free solution phases is to be envisaged. For any exchange of ligand and possibly also water (the basic solvent) there must be no change of the total Gibbs en-

ergy. Thus the relevant chemical potentials are necessarily equal everywhere. This implies a definite functional relationship

$$r = f(c_f, A^*) \quad \text{(A2)}$$

The present two independent variables will also determine the level of any other intensive variable of state, e.g. that of the surface pressure π. Naturally one may invert the given functional relationships by exchanging variables at discretion, for instance c_f with r and A^* with π.

The chemical potential of water as the basic solvent will be that of pure water, μ_o^* (except for extremely high concentrations of ligand in the free solution). This does then apply to any bound water, too. Since μ_o^* is independent of any n_i ($i \neq 0$) the μ_i will not depend on n_o (because of $\partial\mu_i/\partial n_o = \partial\mu_o^*/\partial n_i = 0$!). In other words, changes of bound water do not affect the partitioning equilibrium.

References

[1] G. Scatchard, Ann. New York Acad. Sci. 51 (1949) 660–672.
[2] I.M. Klotz, Science 217 (1982) 1247–1249.
[3] G. Schwarz, Biophys. Struct. Mechanism 2 (1976) 1–12.
[4] J.D. McGhee, P.H. von Hippel, J. Mol. Biol. 86 (1974) 469–489.
[5] G. Schwarz, S. Stankowski, Biophys. Chem. 10 (1979) 173–181.
[6] G. Schwarz, T.J. Gilligan III, Biochemistry 16 (1977) 2835–2840.
[7] S.J. Singer, G.L. Nicolson, Science 175 (1972) 720–731.
[8] W. Bujalowski, T.M. Lohman, Biochemistry 26 (1987) 3099–3106.
[9] G. Schwarz, H. Gerke, V. Rizzo, S. Stankowski, Biophys. J. 52 (1987) 685–692.
[10] F. Watanabe, G. Schwarz, J. Mol. Biol. 163 (1983) 485–498.
[11] G. Schwarz, F. Watanabe, J. Mol. Biol. 163 (1983) 467–484.
[12] G. Schwarz, S. Stankowski, V. Rizzo, Biochim. Biophys. Acta 861 (1986) 141–151.
[13] V. Rizzo, S. Stankowski, G. Schwarz, Biochemistry 26 (1987) 2751–2759.
[14] G. Schwarz, G. Beschiaschvili, Biochim. Biophys. Acta 979 (1989) 82–90.
[15] S. Rex, G. Schwarz, Biochemistry 37 (1998) 2336–2345.
[16] G. Schwarz, U. Blochmann, FEBS Lett. 318 (1993) 172–176.
[17] N. Hellmann, G. Schwarz, Biochem. Biophys. Acta 1369 (1998) 267–277.
[18] A. Arbuzova, G. Schwarz, Biochem. Biophys. Acta 1420 (1999) 139–152.
[19] N. Hellmann, Ph.D. Thesis, University of Basel, 1995.
[20] G. Schwarz, S.E. Taylor, Biophys. J. 76 (1999) 3167–3175.
[21] I. Weis, P.B. Welzel, G. Bähr, G. Schwarz, Chem. Phys. Lipids 105 (2000) 1–8.